Control and Cybernetics

vol. **37** (2008) No. 4

Topological sensitivity analysis for elliptic problems on graphs* †

by

Günter Leugering[1] and Jan Sokolowski[2]

[1]Lehrstuhl für Angewandte Mathematik II,
Friedrich-Alexander-University Erlangen-Nuremberg
Martensstr. 3, D-91058 Erlangen, Germany

[2]Institut Elie Cartan, Laboratoire de Mathématiques,
Université Henri Poincaré Nancy I,
B.P. 239, 54506 Vandouevre les Nancy Cedex, France
e-mail: leugering@am.uni-erlangen.de, Jan.Sokolowski@iecn.u-nancy.fr

Abstract: We consider elliptic problems on graphs under given loads and bilateral contact conditions. We ask the question: which graph is best suited to sustain the loads and the constraints. More precisely, given a cost function we may look at a multiple node of the graph with edge degree q and ask as to whether that node should be resolved into a number of nodes of edge degree less than q, in order to decrease the cost. With this question in mind, we are looking into the sensitivity analysis of a graph carrying a second order elliptic equation with respect to changing its topology by releasing nodes with high edge degree or including an edge. With the machinery at hand developed here, we are in the position to define the topological gradient of an elliptic problem on a graph.

Keywords: differential equations on metric graphs, obstacles, topology optimization, asymptotic analysis.

1. Introduction

Topological derivatives are important in dealing with topology and shape optimization. The reason for this fact is that homeomorphic variations of the domains will not allow for topology changes. Thus, if one considers a shape optimization problem and starts with a simply connected set, say, then all admissible variations will produce simply connected sets. If, therefore, an optimal shape would necessitate digging a hole into the domain, then it would not be possible to do this with the kind of domain variations mentioned. Topological

*We gratefully acknowledge the support of the DAAD PROCOPE program
†Submitted: January 2008; Accepted: September 2008.

gradients are a key ingredient in topology optimization, the boundary between these disciplines becoming increasingly floating. For a number of problems the notion of topological derivatives has been introduced, and examples for such gradients have been reported in the literature. The list of problems considered comprises elliptic problems in two and three dimensions with and without obstacles, the equations of elasticity and the Helmholtz equation, see Sokolowski and Zochowski (1999), Amstutz (2003), Allaire et al. (2004), Masmoudi et al. (2005), Novotny et al. (2007) and others, together with the references therein.

However, the topological gradient is more a qualitative tool than a quantitative one: it helps to indicate where a hole has to be located. The actual optimization of the domain is then subject to shape-sensitivities.

Topology optimization for graph-like problems has been considered in the engineering literature for a long time, see Rozvany (1998) as an example. Truss optimization has also been the focus of many mathematical papers. In truss topology optimization one typically considers a sizing problem where the thickness of an individual bar may be set to zero. In an early paper, Kočvara and Zowe (1996), where, after a proper sizing optimization is performed on a truss, the positions of the nodes are subject to changes, the authors considered a non-smooth two-level problem. However, such truss problems do not describe flexible systems as they use rod-models instead of flexible beam models, nor do they consider 1-d elasticity models other than their finite element representation, which leads to edge-wise linear functions on a graph and hence to a discrete graph problem. The method used there typically comes down to selecting rod elements out of a complete graph in order to decrease a given cost (the typical choice being the compliance). See Mróz and Bojczuk (2003) for graph problems including more general structural elements. We, instead aim at metric graph structures which are locally described by partial differential equations along the edges of the underlying graph. In this paper we confine ourselves to the second order equations which are representative of 1-d elasticity. Timoshenko- and Euler-Bernoulli beams will be discussed in a forthcoming publication.

Similar to Kočvara and Zowe (1996), de Wolf (1996) considered a flow network with simplified flow conditions and investigated topological sensitivities of the minimal resistance network. Again, the problem was treated as a bilevel non-smooth optimization problem. Finally, in a recent paper Durand (2006) considered optimal branching in biological networks and reestablished a Murray-type law. A general theory of abstract 'irrigational networks' has been recently provided by Brenot, Casselles and Morel (2007/2008).

Networks carrying dynamics appear in many applications, such as neuronal dynamics, waste-water management, blood flow, micro-flows, gas- and traffic networks and many more. In all these applications optimization of the topology of the graph is crucial. Thus, it appears reasonable to approach this kind of problem with a topological gradient calculus.

To the best knowledge of the authors, topological gradients for partial differential equations on graphs have not been considered in the literature. Therefore

the major goal of this contribution is to develop the necessary tools towards shape and topology optimization for PDEs on graphs.

The first author has been working on partial differential equations on networked domains during the last 10 years. See the monographs by Lagnese, Leugering and Schmidt (1994) and Lagnese and Leugering (2004) for further reference on the modeling of such problems. For the sake of self-consistency we introduce the models below.

The paper is organized as follows. In the second section we provide preliminaries on elliptic problems on graphs. The third section is devoted to the Steklov-Poincaré operator on the graph. In the fourth section we develop the asymptotic expansions for the problems on graphs with a hole. The last section will be devoted to asymptotic expansions of the energy and a tracking functional.

2. Preliminaries

We consider a simple planar graph $(V, E) = G$ in $\mathbf{R}^2$, with vertices $V = \{v_J | J \in \mathcal{J}\}$ and edges $E = \{e_i | i \in \mathcal{I}\}$. Let $m = |\mathcal{J}|$, $n = \|\mathcal{I}\|$ be the numbers of vertices and edges, respectively. In general, the edge-set may be a collection of smooth curves in $\mathbf{R}^2$, parametrized by their arc lengths. The restriction to planar graphs and *straight edges* is for the sake of simplicity only. The more general case, which is of course also interesting in the combination of shape and topology optimization, can also be handled. However, this is beyond these notes.

We associate to the edge e_i the unit vector $\mathbf{e}_i$ aligned along the edge. $\mathbf{e}_i^{\perp}$ denotes the orthogonal unit vector. Given a node v_J we define

$$\mathcal{I}_J := \{i \in \mathcal{I} | e_i \text{ is incident at } v_J\}$$

the incidence set, and $d_J = |\mathcal{I}_J|$ the edge degree of v_J. The set of nodes splits into simple nodes $\mathcal{J}_S$ and multiple nodes $\mathcal{J}_M$ according to $d_J = 1$ and $d_J > 1$, respectively. On G we consider a vector-valued function r representative of the displacement of the network (see Fig. 1)

$$r : G \to \mathbf{R}^{np} := \Pi_{i \in \mathcal{I}}^{p_i} \mathbf{R},\ p_i \geq 1\, \forall i. \tag{1}$$

The numbers p_i represent the degrees of freedom of the physical model used to describe the behavior of the edge with number i. For instance, $p = 1$ is representative of a heat problem, whereas $p = 2, 3$ is used in an elasticity context on graphs in two or three dimensions. The $p_i's$ may change in the network in principle. However, in this paper we insist on $p_i = p = 2, \forall i$. See Lagnese, Leugering and Schmidt (1994) and Lagnese and Leugering (2004) for details on the modeling.

Once the function r is understood as being representative of, say, a deformation of the graph, we may localize it to the edges

$$r_i := r|_{e_i} : [\alpha_i, \beta_i] \to \mathbf{R}^p,\ i \in \mathcal{I}, \tag{2}$$

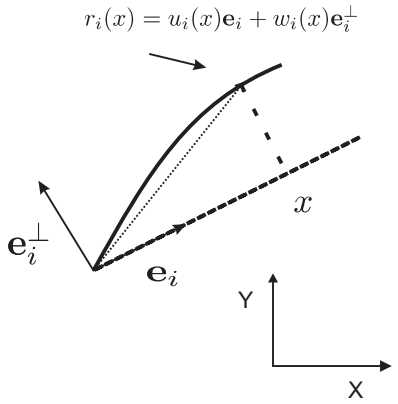

Figure 1. Representation of planar displacement

where e_i is parametrized by $x \in [\alpha_i, \beta_i] =: I_i, 0 \leq \alpha_i < \beta_i$, $\ell_i := \beta_i - \alpha_i$, see Fig. 1

We introduce the incidence relation

$$d_{iJ} := \begin{cases} 1 & \text{if } e_i \text{ ends at } v_J \\ -1 & \text{if } e_i \text{ starts at } v_J. \end{cases}$$

Accordingly, we define

$$x_{iJ} := \begin{cases} 0 & \text{if } d_{iJ} = -1 \\ \ell_i & \text{if } d_{iJ} = 1. \end{cases}$$

We will use notation $r_i(v_J)$ instead of $r_i(x_{iJ})$. In order to represent the material considered on the graph, we introduce stiffness matrices

$$K_i := h_i[(1 - \frac{1}{s_i})I + \frac{1}{s_i}\mathbf{e}_i\mathbf{e}_i^T]. \tag{3}$$

Obviously, the longitudinal stiffness is given by h_i, whereas the transverse stiffness is given by $h_i(1 - \frac{1}{s_i})$. This can be related to 1-d analoga of the Lamé parameters. We introduce Dirichlet and Neumann simple nodes as follows. As the displacements and, consequently, the forces are vectorial quantities, we may consider nodes, where the longitudinal (or tangential) displacement or forces are kept zero, while the transverse displacements of forces are not constrained, and the other way round. We thus define

$$\mathcal{J}_D^t := \{J \in \mathcal{J}_S | r_i(v_J) \cdot \mathbf{e}_i = 0\}$$
$$\mathcal{J}_D^n := \{J \in \mathcal{J}_S | r_i(v_J) \cdot \mathbf{e}_i^\perp = 0\}$$
$$\mathcal{J}_N^t := \{J \in \mathcal{J}_S | d_{iJ} K_i r_i'(v_J) \cdot \mathbf{e}_i = 0\}$$
$$\mathcal{J}_N^n := \{J \in \mathcal{J}_S | d_{iJ} K_i r_i'(v_J) \cdot \mathbf{e}_i^\perp = 0\}.$$

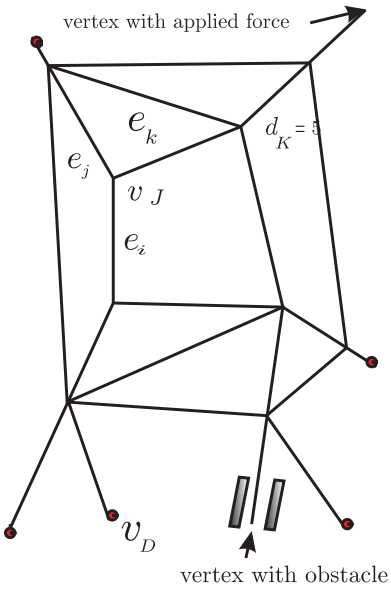

Figure 2. A general graph

Notice that these sets are not necessarily disjoint. Obviously, the set of completely clamped vertices can be expressed as

$$\mathcal{J}_D^0 := \mathcal{J}_D^t \cap \mathcal{J}_D^n. \tag{4}$$

Similarly, a vertex with completely homogenous Neumann conditions is expressed as $\mathcal{J}_N^n \cap \mathcal{J}_N^t$. At tangential Dirchlet nodes in $\mathcal{J}_D^t$ we may, however, consider normal Neumann-conditions as in $\mathcal{J}_N^n$ and so on. In particular, in this paper we will consider bilateral contact conditions for the displacements at simple Dirichlet nodes, see Fig. 2. For the sake of simplicity we concentrate on such obstacles with respect to the transverse displacement only,

$$\tilde{\mathcal{J}}_D^c := \{J \in \mathcal{J}_S | r_i(v_J) \cdot \mathbf{e}_i^\perp \in [a_i, b_i]\}, \tag{5}$$

where $a_i \leq b_i$ for all $i \in \mathcal{I}_D,\ D \in \mathcal{J}_D^c$.

We may then consider bilaterally constrained vertices where the tangential force is zero, i.e. $\mathcal{J}_D^c \cap \mathcal{J}_N^t$ or those with zero longitudinal displacement, i.e. $\mathcal{J}_D^c \cap \mathcal{J}_D^t$. The most general treatment would obscure the presentation, and we thus restrict ourselves to the latter case. Thus, we always assume that a simple vertex under bilateral constraints admits only zero tangential forces. We may therefore define

$$\mathcal{J}_D^c := \left\{J \in \mathcal{J}_S | r_i(v_J) \cdot \mathbf{e}_i^\perp \in [a_i, b_i],\ d_{iJ} K_i r_i'(v_J) \cdot \mathbf{e}_i = 0\right\}. \tag{6}$$

In this paper we do not consider constraints around multiple joints which would restrict the motion of such a joint, say, to a box. Again, the more general situation can be handled with the analysis presented here. The basic assumption at a multiple node is that the deformation r is continuous across the joint. In truss design this is not the case, and consequently pin-joints are considered, albeit on a discrete level. One may consider pin-joints for networks of beams also on the continuous level, as in Lagnese, Leugering and Schmidt (1994) and Lagnese and Leugering (2004). In this paper we restrict ourselves to 'rigid' joints in the sense that the angles between edges in their reference configuration remain fixed. The continuity is expressed simply as

$$r_i(v_J) = r_j(v_J), \quad i,j \in \mathcal{I}_J,\ J \in \mathcal{J}_M.$$

We consider the energy of the system

$$\mathcal{E}_0 := \frac{1}{2}\sum_{i\in\mathcal{I}} \int_0^{\ell_i} K_i r_i' \cdot r_i' + c_i r_i \cdot r_i dx \tag{7}$$

where the primes denote the derivative with respect to the running variable x_i, c_i represents an additional spring stiffness term or an elastic support.

In order to analyze the problem, we need to introduce a proper energy space

$$\mathcal{V} := \{r : G \to \mathbf{R}^{np} | r_i \in H^1(I_i) \tag{8}$$

$$r_i(v_D) = 0,\ i \in \mathcal{I}_D,\ D \in \mathcal{J}_D^0 \tag{9}$$

$$r_i(v_J) = r_j(v_J),\ \forall i,j \in \mathcal{I}_J,\ J \in \mathcal{J}_M\}. \tag{10}$$

$\mathcal{V}$ is clearly a Hilbert space in

$$\mathcal{H} := L^2(0,\ell_i)^{np}. \tag{11}$$

We introduce the bilinear form on $\mathcal{V} \times \mathcal{V}$

$$a(r,\phi) := \sum_{i\in\mathcal{I}} \int_0^{\ell_i} [K_i r_i' \cdot \phi_i' + c_i r_i \cdot \phi_i] dx. \tag{12}$$

Let now the distributed and boundary forces, f_i, g_J be given along the edge e_i and at the node v_J, respectively, which define a continuous linear functional in $\mathcal{V}$

$$L(\phi) := \sum_{i\in\mathcal{I}^f} \int_0^{\ell_i} f_i \cdot \phi_i dx + \sum_{J\in\mathcal{J}_N^g} g_J \cdot \phi_{\hat{i}J}(v_J), \tag{13}$$

where $\hat{i}$ indicates that the simple nodes have just one incident edge, and where $f_i \in H^1(0,\ell_i)^*$. We now consider minimizing the energy over the set of constrained displacements. To this end we introduce the convex and closed (and

hence weakly closed) set

$$\mathcal{K} := \mathcal{V} \cap \{(r_i)_{i=1}^n | r_i(v_D) \cdot \mathbf{e}_i^\perp \in [a_i, b_i],\ i \in \mathcal{I}_D,\ D \in \mathcal{J}_D^c\}. \tag{14}$$

The Ritz-approach to deriving the problem now can be stated as follows

$$\min_{r \in \mathcal{K}} \frac{1}{2} a(r, r) - L(r). \tag{15}$$

That this convex optimization problem admits a unique solution is then proved by standard arguments. The classical first order necessary optimality conditions then read as follows:

$$\sum_{i=1}^n \int_0^{\ell_i} [K_i r_i' \cdot (\hat{r}_i' - r_i') + c_i r_i \cdot (\hat{r}_i - r_i)] dx - \sum_{i=1}^n \int_0^{\ell_i} f_i \cdot (\hat{r}_i - r_i) dx \geq 0,\ \forall \hat{r} \in \mathcal{K}. \tag{16}$$

In order to explore this variational inequality, we introduce active and inactive sets with respect to the bilateral obstacles.

$$\begin{aligned} \mathcal{A}^u &:= \{i | i \in \mathcal{I}_D,\ D \in \mathcal{J}_D^c,\ r_i(v_D) \cdot \mathbf{e}_i^\perp = b_i\} \\ \mathcal{A}^\ell &:= \{i | i \in \mathcal{I}_D,\ D \in \mathcal{J}_D^c,\ r_i(v_D) \cdot \mathbf{e}_i^\perp = a_i\} \\ \mathcal{A}^0 &:= \{i | i \in \mathcal{I}_D,\ D \in \mathcal{J}_D^c,\ a_i < r_i(v_D) \cdot \mathbf{e}_i^\perp < a_i\}. \end{aligned} \tag{17}$$

In order to define proper variations in (16), we introduce the Hilbert space

$$\mathcal{V}^0 = \{\phi \in \mathcal{V} | \phi_i(v_D) \cdot \mathbf{e}_i^\perp = 0,\ i \in \mathcal{I}_D,\ D \in \mathcal{J}_D^c\}. \tag{18}$$

Obviously, if $r \in \mathcal{K}$ then $\hat{r} = r + \phi \in \mathcal{K},\ \forall \phi \in \mathcal{V}^0$. Taking these variations we obtain from (16) the following variational equation

$$\sum_{i=1}^n \int_0^{\ell_i} [K_i r_i' \cdot \phi_i' + c_i r_i \cdot \phi_i - f_i \cdot \phi_i] dx = 0,\ \ \forall \phi \in \mathcal{V}^0. \tag{19}$$

This variational problem, in turn, can be further analyzed by integration by parts (if additional H^2-regularity holds) in order to obtain

$$\begin{aligned} &\sum_{J \in \mathcal{J}_D^c} d_{\hat{i}J} [K_i r_i'(v_J) \cdot \mathbf{e}_i][\phi_i(v_J) \cdot \mathbf{e}_i] \\ &\quad + \sum_{J \in \mathcal{J}_N} d_{\hat{i}J} K_i r_i'(v_J) \phi_{\hat{i}}(v_J) - \sum_{J \in \mathcal{J}_N} g_J \cdot \phi_{\hat{i}}(v_J) \\ &\quad + \sum_{J \in \mathcal{J}_M} \sum_{i \in \mathcal{I}_J} d_{iJ} K_i r_i'(v_J) \cdot \phi_i(v_J) \\ &\quad + \sum_{i=1}^n \int_0^{\ell_i} \{-K_i r_i'' + c_i r_i - f_i\} \cdot \phi_i dx = 0,\ \forall \phi \in \mathcal{V}^0. \end{aligned} \tag{20}$$

Now (20) clearly implies the strong formulation of the problem:

$$\begin{aligned}
&-K_i r_i'' + c_i r_i = f_i \quad \text{in } (0,\ell_i)\\
&\sum_{J\in\mathcal{J}_M}\sum_{i\in\mathcal{I}_J} d_{iJ}K_i r_i'(v_J) = 0, \quad J\in\mathcal{J}_M\\
&d_{iN}K_i r_i'(v_N) = g_N,\ i\in\mathcal{I}_N,\ N\in\mathcal{J}_N\\
&K_i r_i'(v_D)\cdot\mathbf{e}_i = 0,\ i\in\mathcal{I}_D,\ D\in\mathcal{J}_D^c.
\end{aligned} \tag{21}$$

We now concentrate on the active and inactive sets. We may take variations in (16) as follows:

$$\begin{aligned}
&\hat r_i = r_i + \psi_i,\ \psi\in\mathcal{V},\ \psi_i(v_D) = 0,\ i\in\mathcal{I}_D,\ D\in\mathcal{J}_D^c\\
&\qquad i\in\mathcal{A}^u: \quad \psi_i(v_D)\cdot\mathbf{e}_i^\perp \le 0\\
&\qquad i\in\mathcal{A}^l: \quad \psi_i(v_D)\cdot\mathbf{e}_i^\perp \ge 0\\
&\qquad i\in\mathcal{A}^o: \quad \psi_i(v_D)\cdot\mathbf{e}_i^\perp = \pm\varepsilon,\ \varepsilon \text{ small.}
\end{aligned} \tag{22}$$

Obviously, taking variations in the inactive case, we obtain $K_i r_i'(v_D)\cdot\mathbf{e}_i^\perp = 0$ which together with $(21)_4$ gives

$$K_i r_i'(v_D) = 0 \quad i\in\mathcal{A}^o. \tag{23}$$

In the active cases we get

$$d_{iD}K_i r_i'(v_D)\cdot\mathbf{e}_i^\perp[\psi_i(v_D)\cdot\mathbf{e}_i^\perp] \ge 0, \quad i\in\mathcal{A}^u\cup\mathcal{A}^l \tag{24}$$

and hence

$$\begin{aligned}
&d_{iD}K_i r_i'(v_D)\cdot\mathbf{e}_i^\perp \le 0, \quad i\in\mathcal{A}^u\\
&d_{iD}K_i r_i'(v_D)\cdot\mathbf{e}_i^\perp \ge 0, \quad i\in\mathcal{A}^l.
\end{aligned} \tag{25}$$

Putting all together ((21),(25), (23) and the conditions involved in $\mathcal{V}$) we obtain the strong formulation of (16)

$$\left\{\begin{aligned}
&-K_i r_i'' + c_i r_i = f_i,\ \forall i\in\mathcal{I}\\
&r_i(v_D) = 0,\ i\in\mathcal{I}_D,\ D\in\mathcal{J}_D\\
&d_{iD}K_i r_i'(v_N)\cdot\mathbf{e}_i = 0,\ i\in\mathcal{I}_D,\ D\in\mathcal{J}_D^c\\
&d_{iN}K_i r_i'(v_N) = g_J,\ i\in\mathcal{I}_N,\ N\in\mathcal{J}_N\\
&r_i(v_J) = r_j(v_J),\ \forall i,j\in\mathcal{I}_J,\ J\in\mathcal{J}_M\\
&\sum_{i\in\mathcal{I}_J} d_{iJ}K_i r_i'(v_J) = 0,\ J\in\mathcal{J}_M\\
&a_i \le r_i(v_D)\cdot\mathbf{e}_i^\perp \le b_i,\ i\in\mathcal{I}_D,\ D\in\mathcal{J}_D^c\\
&K_i r_i'(v_D)\cdot\mathbf{e}_i^\perp = 0 \quad i\in\mathcal{A}^o\\
&d_{iD}K_i r_i'(v_D)\cdot\mathbf{e}_i^\perp \le 0, \quad i\in\mathcal{A}^u\\
&d_{iD}K_i r_i'(v_D)\cdot\mathbf{e}_i^\perp \ge 0, \quad i\in\mathcal{A}^l
\end{aligned}\right. \tag{26}$$

where $f_i = 0,\ i\in\mathcal{I}\setminus\mathcal{I}^f$, $g_N = 0,\ J\in\mathcal{J}_N\setminus\mathcal{J}_N^g$. Notice that (26), line 6, is an example of the classical Kirchhoff condition known from electrostatics. See Lagnese, Leugering and Schmidt (1994) and Lagnese and Leugering (2004) for the case without obstacles.

3. Steklov-Poincaré operators on graphs

In order to proceed with the introduction of a topological gradient, we consider a multiple node $v_J^0,\ J \in \mathcal{J}_M$. Let the edge degree d_J^0 be greater or equal to three, thus we do not consider a serial junction. Ultimately we would like to cut out a star-subgraph

$$\mathcal{S}^{J^0} := \{e_i | i \in \mathcal{I}_{J^0}\} \subset E,\ (S^{J^0}, v_{J^0}) = G_{J^0} \subset G \tag{27}$$

and connect the adjacent nodes, see Fig. 3. This we consider as digging a hole into the given graph.

We would like to use Steklov-Poincaré operators (Dirchlet-to-Neumann maps) in order to decompose the entire graph into a subgraph and the remaining network (the exterior). In order to do this we pick Dirichlet-values at the simple vertices of the subgraph obtained by the 'cuts' and evaluate the corresponding Neumann-data there by solving the problem on the subgraph. This constitutes the Steklov-Poincaré operator for the subgraph. By a common argument one can then read in the information corresponding to the subgraph by taking the Steklov-Poincaré-data as Neumann inputs at the simple nodes of the remaining graph, (see the next section for details). This decomposition method applies to any subgraph. Thus the 'effect' of the subgraph can be represented in the context of the overall problem by the way of the Steklov-Poincaré operator corresponding to the subgraph. In order to be able to handle holes with varying sizes, we consider decomposing the graph into an exterior part and a subgraph containing the node v_{J^0} to be cut out. That node is considered together with its adjacent edges, however with edge-lengths ρ_i. The obtained star-graph, in turn, is then cut out of the subgraph. Therefore, we obtain the analogue of a ring-like subgraph, which constitutes the Steklov-Poincaré subgraph. See Fig. 3 for a typical general situation and Fig. 4 for the exemplary local handling of subgraph removal.

In order to simplify the notation, and in fact without loss of generality, we may consider the subgraph (from which the hole is then subsequently removed) as a star with edge degree $d_J(v_{J^0}) = q$.

We are led to study the following subproblem

$$\begin{cases} -K_i r_i'' + c_i r_i = f_i,\ i \in \mathcal{I}_{J^0} \\ r_i(v_{J^0,i}) = u_i,\ i \in \mathcal{I}_{J^0} \\ r_i(v_{J^0}) = r_j(v_{J^0}),\ \forall i,j \in \mathcal{I}_{J^0} \\ \sum\limits_{i \in \mathcal{I}_J} d_{iJ} K_i r_i'(v_{J^0}) = 0, \end{cases} \tag{28}$$

where $v_{J_i^0} = v_{J^0,i}$ are the nodes adjacent to v_J, see Fig. 4.

We assume for simplicity that v_{J^0} is an interior node with edge degree q such that its adjacent nodes are not simple. Problem (28) admits a unique solution $r^{i,0},\ i = 1, \dots q$. We consider the Dirichlet-Neumann-map or the Steklov-Poincaré-map

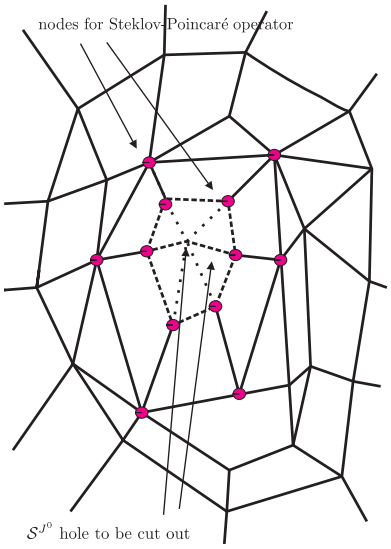

Figure 3. Graph with star-like subgraph to be cut out

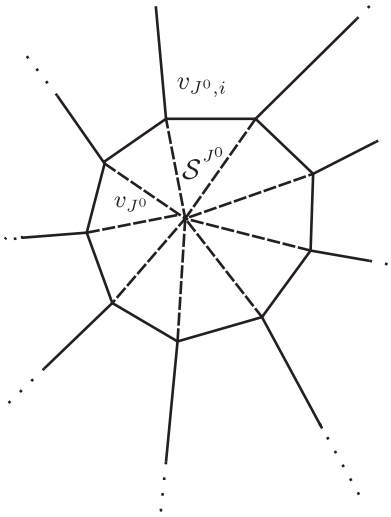

Figure 4. A star-like subgraph

$$\begin{cases} S_{J^0} : \mathbf{R}^{qp} \to \mathbf{R}^{qp} \\ S^i_{J^0} := d_{iJ} K_i r'_{i,0}(v_{J^0}, i),\ i \in \mathcal{I}_{J^0}. \end{cases} \tag{29}$$

In order to simplify notation we may assume that the nodes $v_{J^0,i}$, which are the nodes incident at v_{J^0}, have edge degree ≥ 3 in G, such that after cutting the corresponding edges out of G they are still multiple, but now in $G \setminus G_{J^0}$.

The relevance of the Steklov-Poincaré map in this context becomes apparent when we consider the overall problem. Indeed, we solve the problem (28), generate the Neumann data (29) and integrate those into the system with the hole as follows

$$\begin{cases} -K_i r_i'' + c_i r_i = f_i,\ \forall i \in \mathcal{I} \\ r_i(v_D) = 0,\ i \in \mathcal{I}_D,\ D \in \mathcal{J}_D \\ d_{iD} K_i r_i'(v_N) \cdot \mathbf{e}_i = 0,\ i \in \mathcal{I}_D,\ D \in \mathcal{J}_D^c \\ d_{iJ} K_i r_i'(v_N) = g_J,\ i \in \mathcal{I}_N,\ N \in \mathcal{J}_N \\ r_i(v_J) = r_j(v_J),\ \forall i,j \in \mathcal{I}_J,\ J \in \mathcal{J}_M \setminus \mathcal{J}_S^0 \\ \sum\limits_{i \in \mathcal{I}_J} d_{iJ} K_i r_i'(v_J) = 0,\ J \in \mathcal{J}_M \setminus \mathcal{J}_S^0 \\ r_k(v_J) = r_\ell(v_J) = r_i(v_{J^0,i})\ \forall k,\ell \in \mathcal{I}_{J_S^0},\ i \in \mathcal{I}_{J^0} \\ \sum\limits_{j \in \mathcal{I}_{J_i^0}} d_{j,J_i^0} K_j r_j'(v_{J^0,i}) + S^i_{J^0}(r_i(v_{J^0,i})) = 0,\ i \in \mathcal{I}_{J^0} \\ a_i \leq r_i(v_D) \cdot \mathbf{e}_i^\perp \leq b_i,\ i \in \mathcal{I}_D,\ D \in \mathcal{J}_D^c \\ K_i r_i'(v_D) \cdot \mathbf{e}_i^\perp = 0 \quad i \in \mathcal{A}^o \\ d_{iD} K_i r_i'(v_D) \cdot \mathbf{e}_i^\perp \leq 0,\ \ i \in \mathcal{A}^u \\ d_{iD} K_i r_i'(v_D) \cdot \mathbf{e}_i^\perp \geq 0,\ \ i \in \mathcal{A}^l \end{cases}, \tag{30}$$

where $S^i_{J^0}(r_{\hat{j}}(v_{J^0,i}))_i$ is the Steklov-Poincaré-map applied to the nodal data at $v_{J^0,i}$. The problem (30) is equivalent to the original problem (26). Obviously, there is nothing special about cutting out a star-subgraph. One may as well cut out any subgraph, solve the corresponding Steklov-Poincaré problem, and read it into the graph problem with the 'hole'. The procedure itself is also completely natural in most of the known domain decomposition techniques. See Lagnese and Leugering (2004) for domain decomposition techniques in the context of optimal control problems on networked domains.

4. Stars with a hole

We consider a star-graph G_{J^0} with q edges and center at the node v_{J^0}. As has been seen in the previous section, we may consider this problem completely independently of the original graph. In particular, we may without loss of generality assume that the edges e_i stretch from the center to the simple boundary nodes, which we will label from 1 to q. By this assumption we consider the

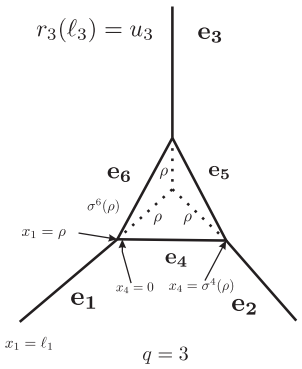

Figure 5. Cutting a hole into star-like subgraph

multiple node at the center as being reached at $x = 0$ for all outgoing edges. Thus, the data u_i are picked up at the ends $x = \ell_i$,

$$\begin{cases} -K_i r_i'' + c_i r_i = f_i,\ i \in \mathcal{I} \\ r_i(\ell_i) = u_i,\ i = 1, \dots, q \\ r_i(0) = r_j(0),\ \forall i, j = 1, \dots, q \\ \sum\limits_{i=1}^{q} K_i r_i'(0) = 0. \end{cases} \tag{31}$$

We are going to cut out the center and connect the corresponding cut-nodes via a circuit as seen in Fig. 5. In general, we have numbers $\rho_i \in [0, \ell_i),\ i = 1, \dots, q$, which are taken to be the lengths of the edges that are cut out. Thus, the remaining edges have lengths $\ell_i - \rho_i$. At $x = \rho_i$ we create a new multiple node v_i. We connect these nodes by edges $e_{q+i},\ i = 1, \dots, q$, with lengths $\sigma^i(\rho_i)$. After that, these nodes receive a new edge degree. In this paper we assume that all these nodes have the same edge degree $d_i = 3$. More complicated cutting procedures can be introduced, but would obscure the ideas of this first paper on topological derivatives of graph problems.

The problem we have to solve is as follows:

$$\begin{cases} -K_i r_i'' + c_i r_i = f_i,\ i \in \mathcal{I} \\ r_i(\ell_i) = u_i,\ i = 1, \dots, q \\ r_i(\rho_i) = r_{q+i}(0) = r_{q+1-i}(\sigma^i(\rho_i)),\ \forall i = 2, \dots, q \\ r_1(\rho_1) = r_{q+1}(0) = r_{2q}(\sigma^{2q}(\rho_{2q})), \\ -K_i r_i'(\rho_i) - K_{q+i} r_{q+i}'(0) + K_{q+i-1} r_{q+i-1}'(\sigma^{q+i-1}(\rho_{q+i-1})) = 0,\ i = 2, \dots, q \\ -K_1 r_1'(\rho_1) - K_{q+1} r_{q+1}'(0) + K_{2q} r_{2q}'(\sigma^{2q}(\rho_{2q})) = 0. \end{cases} \tag{32}$$

We proceed to derive the solutions to (31) and(32), respectively. To this end we look at

$$-K_i r_i'' + c_i r_i = f_i \Leftrightarrow r_i'' = c_i K_i^{-1} r_i - K_i^{-1} f_i$$

and define $A_i := c_i K_i^{-1}$, $F_i := -c_i A_i f_i$. The general solution of the homogeneous equation ($f_i = 0$) is given by

$$r_i^H(x) = \sinh(A_i^{\frac{1}{2}} x) a_i + \cosh(A_i^{\frac{1}{2}} x) b_i, \tag{33}$$

where the sin- and cos-operators are defined via spectral resolution

$$\sinh(A_i^{\frac{1}{2}}(x))\xi = \sum_{j=1}^{p} \sinh(\lambda_{ij}^{\frac{1}{2}} x)(\xi, \phi_{ij})\phi_{ij}, \tag{34}$$

and accordingly for $\cosh(A_i^{\frac{1}{2}}(x))$.

The inhomogeneous equation is then solved by variation of constants as follows

$$r_i^I(x) = A_i^{-\frac{1}{2}} \int_0^x \sinh(A_i^{\frac{1}{2}}(x-s) F_i(s) ds. \tag{35}$$

We will treat the case $f_i = 0$ only. The general case is then a matter of additional but straightforward calculus.

LEMMA 4.1 *The solution r to problem* (31) *with $f_i = 0,\ i = 1, \ldots, q$ is given by*

$$r_i(x) = \sinh((A_i^{\frac{1}{2}})(x)) a_i + \cosh(A_i^{\frac{1}{2}}(x)) b \tag{36}$$

with the coefficient-vectors a_i, b given by

$$a_i = \sinh(A_i^{\frac{1}{2}} \ell_i)^{-1}(u_i - \cosh(A_i^{\frac{1}{2}} \ell_i)$$
$$\cdot(\sum_{i=1}^{q} c_i A_i^{-\frac{1}{2}} \coth A_i^{\frac{1}{2}} \ell_i)^{-1} \sum_{i=1}^{q} c_i A_i^{-\frac{1}{2}} \sinh(A_i^{\frac{1}{2}} \ell_i)^{-1} u_i \tag{37}$$

$$b = (\sum_{i=1}^{q} c_i A_i^{-\frac{1}{2}} \coth(A_i^{\frac{1}{2}} \ell_i))^{-1} \sum_{i=1}^{q} c_i A_i^{-\frac{1}{2}} \sinh(A_i^{\frac{1}{2}} \ell_i)^{-1} u_i. \tag{38}$$

The Steklov-Poincaré map is given by

$$S_{J^0}^i(u) = A_i^{\frac{1}{2}}(\cosh(A_i^{\frac{1}{2}} \ell_i) a_i + \sinh(A_i^{\frac{1}{2}} \ell_i) b) \tag{39}$$

with a_i, b according to (37),(38).

The situation appears to be much simpler in case all material parameters and geometrical data are equal:

$$c_i = 1,\ K_i = Id = A^{\frac{1}{2}},\ \ell_i = \ell,\ f_i = 0, \quad i = 1, \ldots q \tag{40}$$

EXAMPLE 4.1 *Let assumption* (40) *hold true. Then the solution* r *to* (31) *is given by*

$$r_i(x) = \frac{1}{\sinh(\ell)}\sinh(x)(u_i - \frac{1}{q}\sum_{j=1}^{q} u_j) + \frac{1}{\cosh(\ell)}\cosh(x)\frac{1}{q}\sum_{i=1}^{q} u_i. \tag{41}$$

The Steklov-Poincaré map is given by

$$S^i(u)_{J^0} = \coth(\ell)(u_i - \frac{1}{q}\sum_{j=1}^{q} u_j) + \tanh(\ell)\frac{1}{q}\sum_{j=1}^{q} u_j. \tag{42}$$

We proceed to problem (32). Again, we will treat the general case first and will then restrict to assumption (40) in order to better reveal the underlying structure.

We introduce the ansatz for the solution as follows

$$r_i^\rho(x) := \sinh(A_i^{\frac{1}{2}}x)a_i^\rho + \cosh(A_i^{\frac{1}{2}}x)b_i^\rho. \tag{43}$$

From the Dirichlet conditions in $(32)_2$ we infer

$$r_i^\rho(\ell_i) = \sinh(A_i^{\frac{1}{2}}(\ell_i))a_i^\rho + \cosh(A_i^{\frac{1}{2}}(\ell_i))b_i^\rho = u_i,\ i = 1, \dots, q. \tag{44}$$

From the continuity requirement in $(32)_{3,4}$ we obtain

$$\begin{aligned} r_i^\rho(\rho_i) &= \sinh(A_i^{\frac{1}{2}}\rho_i)a_i^\rho + \cosh(A_i^{\frac{1}{2}}\rho_i)b_i^\rho = r_{q+i}^\rho(0) = b_{q+i}^\rho \\ &= r_{q+i-1}^\rho(\sigma^{q+i-1}(\rho_{q+i-1})),\ i = 2, \dots q. \end{aligned} \tag{45}$$

$$\begin{aligned} r_1^\rho(\rho_1) &= \sinh(A_1^{\frac{1}{2}}\rho_1)a_1^\rho + \cosh(A_1^{\frac{1}{2}}\rho_1)b_1^\rho \\ &= r_{q+1}^\rho(0) = b_{q+1}^\rho = r_{2q}^\rho(\sigma^{2q}(\rho_{2q})). \end{aligned} \tag{46}$$

The Kirchhoff conditions in (32) result in

$$\begin{aligned} &-c_i A_i^{-\frac{1}{2}}[\cosh(A_i^{\frac{1}{2}}\rho_i)a_i^\rho + \sinh(A_i^{\frac{1}{2}}\rho_i)b_i^\rho] - c_{q+i}A_{q+i}^{-\frac{1}{2}}a_{q+i}^\rho \\ &\quad + c_{q+i-1}A_{q+i-1}^{-\frac{1}{2}}[\cosh(A_{q+i-1}^{\frac{1}{2}}(\sigma^{q+i-1}(\rho_{q+i-1})))a_{q+i-1}^\rho \\ &\quad\quad + \sinh(A_{q+i-1}^{\frac{1}{2}}(\sigma^{q+i-1}(\rho_{q+i-1})))b_{q+i-1}^\rho] = 0,\ i = 2, \dots, q. \end{aligned} \tag{47}$$

$$\begin{aligned} &-c_1 A_1^{-\frac{1}{2}}[\cosh(A_1^{\frac{1}{2}}\rho_1)a_1^\rho + \sinh(A_1^{\frac{1}{2}}\rho_1)b_1^\rho] - c_{q+1}A_{q+1}^{-\frac{1}{2}}a_{q+1}^\rho \\ &\quad + c_{2q}A_{2q}^{-\frac{1}{2}}[\cosh(A_{2q}^{\frac{1}{2}}(\sigma^{2q}(\rho_{2q})))a_{2q}^\rho \\ &\quad\quad + \sinh(A_{2q}^{\frac{1}{2}}(\sigma^{2q}(\rho_{2q})))b_{2q}^\rho] = 0. \end{aligned} \tag{48}$$

This set of equations (44)–(48) constitutes $4q$ conditions on the $4q$ unknowns $a_i^\rho,\ b_i^\rho,\ i=1,\dots,2q$. The problem is as to whether there is an asymptotic expansion of r_i^ρ in terms of ρ for small $\rho := (\rho_i)_{i=1,\dots,q}$. Notice that the graph with $\rho = 0$ is the original star-graph with q edges, while for every $\rho > 0$ (i.e. $\rho_i > 0$), the graph has $2q$ edges and contains exactly one circuit. We may, of course, also formally start with a star-graph consisting of $2q$ edges with serial joints at $x_i = 0,\ x_{q+i} = \rho_i,\ i = 1,\dots,q$ so that the edges $e_i,\ i = 1,\dots,q$, have length $\ell_i - \rho_i$ to begin with, while the other edges $e_{q+i},\ i = 1,\dots,q$, stretch from the center (at $x_{q+i} = 0$) to the serial nodes at $x_{q+i} = \rho_i$.

Our analysis depends on the expansion of the set of equations (44) to (48) up to second order terms. The asymptotic analysis is based on the expansions of $\sinh(x), \cosh(x)$ on the matrix level. We use the asymptotic expansions in (34) as follows

$$\begin{cases} \sinh(A_i^{\frac{1}{2}}(\sigma^i(\rho_i)))\xi = \sigma^i(\rho_i)A_i^{\frac{1}{2}}\xi + O(\rho_i^2) \\ \cosh(A_i^{\frac{1}{2}}(\sigma^i(\rho_i)))\xi = \xi + O(\rho_i^2). \end{cases} \tag{49}$$

By (44) we have

$$a_i^\rho = (\sin(A_i^{\frac{1}{2}}(\ell_i))^{-1}(u_i - \cosh(A_i^{\frac{1}{2}}(\ell_i))b_i^\rho),\ i = 1,\dots,q. \tag{50}$$

We expand (45) and(46)

$$\begin{aligned} A_i^{\frac{1}{2}}\rho_i a_i^\rho + b_i^\rho &= b_{q+i}^\rho \qquad (51)\\ &= \sigma^{q+i-1}(\rho_{q+i-1})A_{q+i-1}^{\frac{1}{2}}a_{q+i-1}^\rho + b_{q+i-1}^\rho + O(\rho^2),\ i = 2,\dots q. \\ A_1^{\frac{1}{2}}\rho_1 a_1^\rho + b_1^\rho &= b_{q+1}^\rho = \sigma^{2q}(\rho_{2q})A_{2q}^{\frac{1}{2}}a_{2q}^\rho + b_{2q}^\rho + O(\rho^2). \qquad (52) \end{aligned}$$

We now proceed to the Kirchhoff conditions at the multiple nodes (47),(48)

$$\begin{aligned} &-c_i A_i^{-\frac{1}{2}}[a_i^\rho + \rho_i A_i^{\frac{1}{2}}b_i^\rho] - c_{q+i}A_{q+i}^{-\frac{1}{2}}a_{q+i}^\rho \\ &\quad + c_{q+i-1}A_{q+i-1}^{-\frac{1}{2}}[a_{q+i-1}^\rho + \sigma^{q+i-1}(\rho_{q+i-1})A_{q+i-1}^{\frac{1}{2}}b_{q+i-1}^\rho] \\ &\qquad = 0 + O(\rho^2),\ i = 2,\dots,q \end{aligned} \tag{53}$$

and

$$\begin{aligned} &-c_1 A_1^{-\frac{1}{2}}[a_1^\rho + \rho_1 A_1^{\frac{1}{2}}b_1^\rho] - c_{q+1}A_{q+1}^{-\frac{1}{2}}a_{q+1}^\rho \\ &\quad + c_{2q}A_{2q}^{-\frac{1}{2}}[a_{2q}^\rho + \sigma^{2q}(\rho_{2q})A_2^{\frac{1}{2}}b_{2q}^\rho] = 0 + O(\rho^2). \end{aligned} \tag{54}$$

We reformulate the system (51),(52),(53),(54) as follows

$$\begin{aligned}
&\left[A_{i-1}^{\frac{1}{2}}\rho_{i-1} - \tanh(A_{i-1}^{\frac{1}{2}}\ell_{i-1})\right] a_{i-1}^{\rho} - \left[A_i^{\frac{1}{2}}\rho_i - \tanh(A_i^{\frac{1}{2}}\ell_i)\right] a_i^{\rho} \qquad (55)\\
&\quad + \sigma^{q+i-1}(\rho_{q+i-1}) A_{q+i-1}^{\frac{1}{2}} a_{q+i-1}^{\rho}\\
&\quad = \cosh(A_i^{\frac{1}{2}}\ell_i)^{-1} u_i - \cosh(A_{i-1}^{\frac{1}{2}}\ell_{i-1})^{-1} u_{i-1},\ i = 2, \dots, q,\\
&- \left[A_1^{\frac{1}{2}}\rho_1 - \tanh(A_1^{\frac{1}{2}}\ell_1)\right] a_1^{\rho} + \left[A_q^{\frac{1}{2}}\rho_q - \tanh(A_q^{\frac{1}{2}}\ell_q)\right] a_q^{\rho}\\
&\quad + \sigma^{2q}(\rho_{2q}) A_{2q}^{\frac{1}{2}} a_{2q}^{\rho} = \cosh(A_1^{\frac{1}{2}}\ell_1)^{-1} u_1 - \cosh(A_q^{\frac{1}{2}}\ell_q)^{-1} u_q + O(\rho^2),\\
&- \left[c_i A_i^{-\frac{1}{2}} + (\sigma^{q+i-1}(\rho_{q+i-1}) c_{q+i-1} - \rho_i c_i)\tanh(A_i^{\frac{1}{2}}\ell_i)\right] a_i^{\rho} \qquad (56)\\
&\quad - c_{q+i} A_{q+i}^{-\frac{1}{2}} a_{q+i}^{\rho} + c_{q+i-1} A_{q+i-1}^{-\frac{1}{2}} a_{q+i-1}^{\rho}\\
&\quad = -\left(\sigma^{q+i-1}(\rho_{q+i-1}) c_{q+i-1} - \rho_i c_i\right) \cosh(A_i^{\frac{1}{2}}\ell_i)^{-1} u_i,\ i = 2, \dots q,\\
&- \left[c_1 A_1^{-\frac{1}{2}} + (\sigma^{2q}(\rho_{2q}) c_{2q} - \rho_1 c_1)\right] \tanh(A_1^{\frac{1}{2}}\ell_1) a_1^{\rho}\\
&\quad - c_{q+1} A_{q+1}^{-\frac{1}{2}} a_{q+1}^{\rho} + c_{2q} A_{2q}^{-\frac{1}{2}} a_{2q}^{\rho}\\
&\quad = -\left(\sigma^{2q}(\rho_{2q}) c_{2q} - \rho_1 c_1\right) \cosh(A_1^{\frac{1}{2}}\ell_1)^{-1} u_1 + O(\rho^2).
\end{aligned}$$

Now, (55)-(56) constitute a system of $2q$ linear asymptotic equations to order 2 in the $2q$ variables $a_i^{\rho},\ i = 1, \dots, 2q$.

THEOREM 4.1 *The system of equations* (53) *to* (56) *admits a unique solution* $a_i^{\rho},\ i = 1, \dots 2q$. *Moreover, we have the asymptotic expansion*

$$a_i^{\rho} = a_i + O(\rho), \quad i = 1, \dots, q, \tag{57}$$

where a_i *is given by* (37). *There exists a function* $s_i(\cdot)$ *such that*

$$r_i^{\rho}(x) = r_i(x) + O(\rho) s_i(x), \quad i = 1, \dots, q, \tag{58}$$

where r_i *is the solution of the star-graph problem* (31) $\rho = 0$.

Proof. Using equations (51) and (52), taking appropriate differences, we realize that $b_i = \hat{b} + O(\rho)$. This information is inserted into equations (53) and (54). If we write all quantities involving a_i^{ρ} with indices $i = 1 \dots q$ on the left and the other terms on the right side, we obtain after summing up, using a 'telescope-sum', only $O(\rho)$-terms on the right hand side, i.e. we have

$$\sum_{i=1}^{q} c_i A_i^{-\frac{1}{2}} a_i^{\rho} = O(\rho). \tag{59}$$

Then we use the expression (50) for a_i^ρ in (59) to obtain

$$\sum_{i=1}^{q} c_i A_i^{-\frac{1}{2}} \sinh(A_i^{\frac{1}{2}}\ell_i)^{-1} u_i = \left(\sum_{i=1}^{q} c_i A_i^{-\frac{1}{2}} \coth(A_i^{\frac{1}{2}}\ell_i)^{-1} \right) \hat{b}.$$

From this and (38) we see that up to terms of order $O(\rho)$, $\hat{b} = b$. Then a_i^ρ, up to the order $O(\rho)$, are given by a_i in (37). ∎

4.1. Homogeneous networks

In this subsection we consider the network under the assumption (40), i.e. all material and geometrical quantities are the same, and a symmetric hole. Under this assumption the system of equations (55) to (56) reduces to

$$\begin{aligned}
&a_{i-1}^\rho - a_i^\rho - \sigma\rho\coth(\ell) a_{q+i-1}^\rho = -\frac{1+\rho\coth(\ell)}{\sinh(\ell)}(u_i - u_{i-1}) + O(\rho^2), \quad (60)\\
&-a_1^\rho + a_q^\rho - \sigma\rho\coth(\ell) a_{2q} = -\frac{1+\rho\coth(\ell)}{\sinh(\ell)}(u_1 - u_q) + O(\rho^2),\\
&-(1+(\sigma-1)\rho\tanh(\ell))a_i^\rho - a_{q+i}^\rho + a_{q+i-1}^\rho = \frac{1-\sigma}{\cosh(\ell)} u_i + O(\rho^2)\\
&-(1+(\sigma-1)\rho\tanh(\ell))a_1^\rho - a_{q+1}^\rho + a_{2q}^\rho = \frac{1-\sigma}{\cosh(\ell)} u_1 + O(\rho^2),
\end{aligned}$$

where the first and the third equations hold for $i = 2, \ldots, q$, respectively. This system has a very particular structure, which reflects the adjacency structure of the graph. To obtain the direct explicit solution is, nevertheless, a matter of substantial calculations. Instead we look at an example.

EXAMPLE 4.2 *In this example we reduce the graph to a tripod, see Fig. 5. Here we can solve* (60) *analytically an obtain*

$$\begin{aligned}
a_i^\rho = &\frac{1}{\sinh(\ell)}(u_i - \frac{1}{3}\sum_{j=1}^{3} u_j)\\
&+\rho\frac{1}{\cosh(\ell)}\left\{ (1-\frac{1}{3}\sigma)\coth(\ell)^2(u_i - \frac{1}{3}\sum_{j=1}^{3} u_j) \right. \quad (61)\\
&\qquad \left. + (\sigma-1)\frac{1}{3}\sum_{j=1}^{3} u_j \right\} + O(\rho^2),
\end{aligned}$$

$$
\begin{aligned}
b_i^\rho &= \frac{1}{\cosh(\ell)}\frac{1}{3}\sum_{j=1}^{3} u_j \\
&\quad -\rho\frac{\sinh(\ell)}{\cosh(\ell)^2}\left\{\left((1-\frac{1}{3}\sigma)\coth(\ell)^2\right)(u_i-\frac{1}{3}\sum_{j=1}^{3}u_j)\right. \\
&\qquad \left. +(\sigma-1)\frac{1}{3}\sum_{i=1}^{3}u_i\right\}+O(\rho^2),
\end{aligned}
\tag{62}
$$

where $i=1,2,3$.

We also display the coefficients a^ρ_{q+i}, $i=1,2,3$ *in order to reveal the behavior of the edges introduced by cutting the hole:*

$$
a_4^\rho = \frac{1}{3\sinh(\ell)}(u_2-u_1)+\frac{\rho}{3\sinh(\ell)}\big((1-\frac{\sigma}{3})\coth(\ell))(u_2-u_1)\big)+O(\rho^2) \tag{63}
$$

$$
a_5^\rho = \frac{1}{3\sinh(\ell)}(u_3-u_2)+\frac{\rho}{3\sinh(\ell)}\big((1-\frac{\sigma}{3})\coth(\ell))(u_3-u_2)\big)+O(\rho^2) \tag{64}
$$

$$
a_6^\rho = \frac{1}{3\sinh(\ell)}(u_1-u_3)+\frac{\rho}{3\sinh(\ell)}\big((1-\frac{\sigma}{3})\coth(\ell)(u_1-u_3)\big)+O(\rho^2). \tag{65}
$$

The remaining b_{q+i}, $1=1,2,3$ *are of course given by* b_i, $i=1,2,3$ *according to* (51),(52). *This completely determines the solution* $r_i^\rho(x)$, $i=1,\dots,6$. *We list the first three members for easier reference:*

$$
\begin{aligned}
r_i^\rho(x) &= \frac{1}{\sinh(\ell)}\big(u_i-\frac{1}{3}\sum_{j=1}^{3}u_j\big)\sinh(x)+\frac{1}{\cosh(\ell)}\frac{1}{3}\sum_{j=1}^{3}u_j\cosh(x) \\
&\quad +\rho\left\{\frac{1}{\cosh(\ell)}\left[(1-\frac{1}{3}\sigma)\coth(\ell)^2(u_i-\frac{1}{3}\sum_{j=1}^{3}u_j)\right.\right. \\
&\qquad \left.+(\sigma-1)\frac{1}{3}\sum_{j=1}^{3}u_j\right]\sinh(x) \\
&\qquad -\frac{\sinh(\ell)}{\cosh(\ell)^2}\left[(1-\frac{1}{3}\sigma)\coth(\ell)^2(u_i-\frac{1}{3}\sum_{j=1}^{3}u_j)\right. \\
&\quad \left.\left.+(\sigma-1)\frac{1}{3}\sum_{j=1}^{3}u_j\right]\cosh(x)\right\} \quad +O(\rho^2),\ i=1,2,3.
\end{aligned}
\tag{66}
$$

The Steklov-Poincaré-map is then obtained using

$$
\begin{aligned}
(r_i')^\rho(\ell) &= \coth(\ell)(u_i - \frac{1}{3}\sum_{j=1}^{3} u_j) + \tanh(\ell)\frac{1}{3}\sum_{j=1}^{3} u_j \\
&+\rho\left\{(1-\tanh^2(\ell))[(1-\frac{1}{3}\sigma)\coth^2(\ell)(u_i - \frac{1}{3}\sum_{j=1}^{3} u_j)) \right. \\
&\left. + (\sigma-1)\frac{1}{3}\sum_{j=1}^{3} u_j]\right\},\ i = 1,\dots q.
\end{aligned} \tag{67}
$$

It is apparent that (66),(67) *provide the second order asymptotic expansion we were looking for. We consider the following experiment: we apply longitudinal forces* $u_i = ue_i$ *with the same magnitude at the simple nodes of the network. The (outer) edges* $e_i,\ 1 = 1, 2, 3$ *or, respectively the edges of the original star, are given by*

$$
e_1 = (0,1),\ e_2 = (-\frac{\sqrt{3}}{2}, -\frac{1}{2}),\ e_3 = (\frac{\sqrt{3}}{2}, -\frac{1}{2})
$$

which together with the orthogonal complements

$$
e_1^\perp = (-1,0),\ e_2^\perp = (\frac{1}{2}, -\frac{\sqrt{3}}{2}),\ e_3^\perp = (\frac{1}{2}, \frac{\sqrt{3}}{2})
$$

form the local coordinate systems of the edges. Obviously, $\sum_{i=1}^{3} e_i = 0$. *Thus, the solution to the unperturbed problem is given by*

$$
r_i(x) = \frac{1}{\sinh(\ell)} u \sinh(x) e_i. \tag{68}
$$

This is in agreement with the fact that that particular reference configuration is completely symmetric. Now, the solution r_i^ρ *to the perturbed system and* $(r_i')^\rho(\ell)$ *are then given by*

$$
\begin{aligned}
r_i^\rho(x) &= \frac{1}{\sinh(\ell)}\sinh(x) u e_i \\
&\quad +\rho(1-\frac{\sigma}{3})\frac{1}{\sinh(\ell)}\left(\coth(\ell)\sinh(x) - \cosh(x)\right) u e_i \ + O(\rho^2) \\
(r_i)'^\rho(\ell) &= \coth(\ell) u e_i + \rho(\coth(\ell)^2 - 1)(1-\frac{\sigma}{3}) u e_i \ + O(\rho^2).
\end{aligned} \tag{69}
$$

The energy of the unperturbed system is given by

$$
\mathcal{E}_0 = \frac{1}{2}\sum_{i=1}^{3}\int_0^\ell r_i' \cdot r_i' + r_i \cdot r_i dx = \frac{3}{2}\coth(\ell) u^2. \tag{70}
$$

The energy of the perturbed system is given by

$$\mathcal{E}^\rho = \frac{1}{2}\sum_{i=1}^{3}\int_0^{\ell-\rho}[r_i'\cdot r_i' + r_i\cdot r_i]dx + \frac{1}{2}\sum_{i=4}^{6}\int_0^{\sigma\rho}[r_i'\cdot r_i' + r_i\cdot r_i]dx \tag{71}$$

$$= \frac{1}{2}\langle S^\rho u, u\rangle = \frac{1}{2}\langle S^0 u, u\rangle + \rho\frac{1}{2}(1-\frac{\sigma}{3})\left\{((\coth(\ell))^2-1)\right\}u^2 \tag{72}$$

$$= \frac{1}{2}\langle S^0 u, u\rangle + \rho\frac{\sqrt{3}}{2}(\sqrt{3}-1)\sinh(\ell)^{-2}u^2. \tag{73}$$

From these experiments we may draw the conclusion, that nodes of edge degree 3 under symmetric load, where the configuration is at 120° between the edges (this amounts to $\sigma = \sqrt{3}$) are not going to be replaced by a hole, which would, in turn result in three new multiple nodes of edge degree 3. This seems to support the optimality of such graphs as observed by Buttazzo (2005).

REMARK 4.1

1. *Very similar formulae are obtained in the scalar case ($r_i(x) \in \mathbf{R}$, no planar representation!), relevant for instance in problems of heat transfer or electrical currents in networks.*
2. *If the loads are not symmetric, and/or if the geometry of the 'hole' is not uniform, the energy may in fact drop. A more detailed analysis is the subject of a forthcoming paper. It suffices to say here, that nodes with higher edge degree, according to our analysis, are 'more likely' to be released by a hole, as even in the symmetric case the number $\sigma(\rho)$ which measures the new edge-lengths will be less than 1.*
   This is true e.g. for a node with edge degree 6 and beyond. Thus, the total length of the new edges is smaller than the total length of the removed edges. This, in turn, is intuitive with respect to the fact that in the higher-dimensional problem (in 2- or 3-d, no graphs), digging a hole reduces the amount of mass.

EXAMPLE 4.3 *Here we consider the homogeneous situation for a star with edge degree 6 at the multiple node. In this case $\sigma = 1$ for the symmetric situation. See Fig. 6*

We calculate

$$a_1^\rho = \frac{1}{\sinh(\ell)}(u_1 - \frac{1}{6}\sum_{j=1}^{6}u_j) \tag{74}$$

$$+\rho\frac{\cosh(\ell)}{\cosh^2(\ell)-1}\left\{(-u_5-u_3-4u_2-4u_6+10u_1) - 7(u_1-\frac{1}{6}\sum_{j=1}^{6}u_j)\right\}.$$

Notice that the edges 2 and 6 are the 'neighboring' edges of edge 1 in the original star-graph. The other coefficients a_i^ρ, $1 = 2,\ldots,6$ are then obvious.

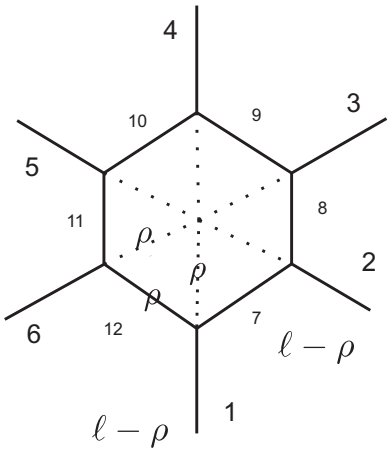

Figure 6. Graph with 'critical' edge degree 6

For the sake of brevity, we only display e.g. a_{12}^{ρ}*:*

$$a_{12}^{\rho} = \frac{1}{12\sinh(\ell)}[5(u_1-u_6)+3(u_2-u_5)+(u_3-u_4)]$$
$$-\rho\frac{\cosh(\ell)}{144(\cosh^2(\ell)-1)}[25(u_1-u_6)-9(u_2-u_5)-7(u_3-u_4)]$$
$$+O(\rho^2). \tag{75}$$

Again, observe that edge 12, in terms of the edges of the original graph, has direct neighbors 1 and 6, the next level is 2 and 5 and finally we have 3 and 4. One realizes a consequent scaling. Also note that $a_i^{\rho} = 0$ *if* u_i *are all equal. This shows that the coefficients* b_i^{ρ} *in that case are independent of* ρ *and thus the energy will not change for this limiting case.*

5. The topological derivative

We are now in the position to define the topological derivative of an elliptic problem on a graph. Let G be a graph, and let $v_J \in \mathcal{J}_M$ be a multiple node with edge degree d_J. Let G_ρ be the graph obtained from G by replacing v_J with a cycle of length $\sum_{i=1}^{d_J} c_i\rho$ with vertices $v_J^1, \dots v_J^{d_J}$ of edge degree 3 each, such that the distance from v_J to v_J^i is equal to ρ. Thus, the number n^ρ of edges of G_ρ is $n + d_J$. Let $\mathcal{J} : G \to \mathbf{R}$ be a functional on the edges of G

$$J(r, r', G) := \sum_{i=1}^{n} \int_0^{\ell_i} F(x, r_i, r_i') \tag{76}$$

and let

$$J(r^\rho,(r^\rho)',G_\rho) := \sum_{i=1}^{n+d_J} \int_0^{\ell_i^\rho} F(x,r_i^\rho,(r_i^\rho)') \tag{77}$$

be its extension to $G\rho$. Assume we have an asymptotic expansion as follows

$$J(r^\rho,(r^\rho)',G_\rho) = J(r,r',G) + \rho\mathcal{T}(v_J) + O(\rho^2) \tag{78}$$

then we define the topological gradient of $J(G_\rho)$ with respect to ρ for $\rho = 0$ at the vertex v_J as follows.

$$\mathcal{T}(v_J) = \lim_{\rho\to 0} \frac{J(r^\rho,(r^\rho)',G_\rho) - J(r,r',G)}{\rho}. \tag{79}$$

We consider the energy functional or, equivalently, the compliance which is the most natural criterion to begin with. There are five such functionals relevant for the analysis of this paper: $E^0(r)$ on the entire graph G , $E^\rho(r^\rho)$ on the entire graph with the hole G^ρ , $E_{CS}(r)$ on the graph $G\setminus\mathcal{S}^{J^0}$, where the star-graph without hole $\mathcal{S}^{J^0}$ has been cut out along edges $e_i,\ i\in\mathcal{I}_{J^0}$, $E_S^0(r;v)$ on the star-graph without hole, and $E_S^\rho(r;v)$ on the star-graph with a hole. Obviously

$$E_S^0(r;u) = \frac{1}{2}\langle S^0u,u\rangle, \tag{80}$$

$$E_S^\rho(r;u) = \frac{1}{2}\langle S^\rho u,u\rangle, \tag{81}$$

$$E^0(r) = E_{CS}(r) + E_S^0(r,r), \quad E^\rho(r^\rho) = E_{CS}(r^\rho) + E_S^\rho(r^\rho,r^\rho), \tag{82}$$

where it is understood that in $E_S^\rho(r^\rho,\cdot)$ and $E_S^0(r,\cdot)$ we insert $u_i = r^\rho(\ell_i)$ and $u_i = r^0(\ell_i)$, respectively. Thus

$$E^\rho(r^\rho) - E^0(r) = \frac{1}{2}\langle S^\rho(\tilde r),\tilde r\rangle - \frac{1}{2}\langle S^0(\tilde r),\tilde r\rangle, \tag{83}$$

where $\tilde r$ solves the problem on $G\setminus\mathcal{S}^{J^0}$ and $u_i = \tilde r_i(\ell_i), i\in\mathcal{I}_{J^0}$. Thus, the asymptotic analysis of the last section carries over to the entire graph. As we have done the complete asymptotic analysis up to order 2 in the homogeneous case only, we consequently dwell on this case now, the more general case will be subject of a forthcoming publication.

5.1. Homogeneous graphs

In order to find an expression of the topological gradient in terms of the solutions r at the node v_{J^0}, the one that is cut out, we need to express the solution in terms of the data u_i.

EXAMPLE 5.1 *We consider the star-graph as above with 3 edges. Obviously*

$$u_i - \frac{1}{3}\sum_{j=1}^{3} u_j = \sinh(\ell) r_i'(0),\ \frac{1}{3}\sum_{j=1}^{3} u_j = \cosh(\ell) r_i(0). \tag{84}$$

Thus using the fact that $\sum_{i=1}^{3} \|u_i - \frac{1}{3}\sum_{j=1}^{3} u_j\|^2 = \sum_{i=1}^{3} \|u_i\|^2 - \frac{1}{3}(\|\sum_{i=1}^{3}\|)^2$ *we can express the bilinear expression* $\langle \mathcal{S}^\rho(u), u\rangle$ *in terms of* $\|r^0(0)\|^2$ *and* $\|(r^0)'(0)\|^2$ *(where we omit the index* 0*) as follows*

$$\begin{aligned}\langle \mathcal{S}_i^\rho(u), u\rangle &= \langle \mathcal{S}_i^0(u), u\rangle \\ &\quad +\rho\left\{(1-\tfrac{1}{3}\sigma)\sum_{i=1}^{3}\|r_i'(0)\|^2 + (\sigma-1)\sum_{i=1}^{3}\|r_i(0)\|^2\right\}.\end{aligned} \tag{85}$$

This says that the energy function in the homogeneous case, when cutting out a symmetric hole e.g. $\sigma^i = \sigma = \sqrt{3},\ i = 1, 2, 3$*, we have*

$$\mathcal{T}_E(r, v_{J^0}) = \frac{1}{2}\left\{(1-\frac{1}{3}\sigma)\sum_{i=1}^{3}\|r_i'(0)\|^2 + (\sigma-1)\sum_{i=1}^{3}\|r_i(0)\|^2\right\}. \tag{86}$$

The situation will be different for such vertices having a higher edge-degree than 6, and those having non-symmetric holes. We expect that such networks are more likely to be reduced to edge-degree 3 by tearing a hole. But this has to be confirmed by more detailed studies.

More general functionals will be considered in a forthcoming publication.

5.2. Sensitivity with respect to edge inclusion

We now consider a different situation, where a node with edge degree $d_J = N$ is transformed into a node of edge degree 3 and one of degree $N-1$ by introduction of a new edge e_{N+1}, see Fig. 7.

We consider this procedure in an explicit example with edge degree 4.

Let, therefore, v_J be a node with edge degree 4. As visualized in Fig. 7, we will introduce an additional new edge e_5^ρ of length $\rho > 0$ which, together, with the two new edges e_1^ρ, e_2^ρ given by

$$\begin{aligned} e_1^\rho &:= \frac{\ell_1 e_1 - \rho e_{N+1}}{\|\ell_1 e_1 - \rho e_{N+1}\|} \\ e_2^\rho &:= \frac{\ell_2 e_1 - \rho e_{N+1}}{\|\ell_2 e_2 - \rho e_{N+1}\|}, \end{aligned} \tag{87}$$

where in our case study below $N = 4$.

The new lengths $\ell - \sigma$ of the edges e_1^ρ, e_2^ρ (we consider a symmetric situation where the new additional edge e_{N+1} equally divides the angle between e_1, e_2 with an inclination α towards the corresponding unit vectors) can be computed by elementary trigonometry. The number σ is then found to be

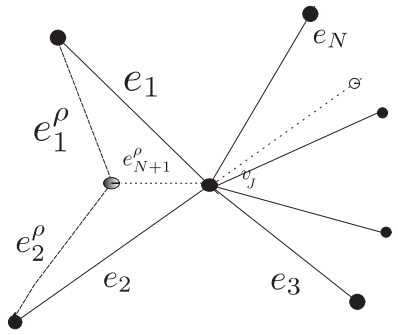

Figure 7. N-node turns into 3-node plus (N+1)-node

$$\sigma = \rho\cos\alpha - \rho^2\frac{1}{2\ell}(1-\frac{1}{\ell}\cos^2\alpha) + O(\rho^3). \tag{88}$$

It is interesting to notice that for $\cos\alpha > \frac{1}{2}$ the new graph has actually a smaller total length. This is in contrast to the standard situation, where cutting out a hole - which in fact implies introducing new the edges forming that hole - has the opposite effect. For the sake of simplicity, we calculate the sensitivities with respect to introducing the new edge of length ρ for the Laplacian on the graph only. Thus, we do not consider an extra stiffening part due to the presence of a term cr_i,

$$\begin{cases} -r_i'' = 0 \quad \text{in } I_i,\ i = 1,\dots,5 \\ r_i(\ell) = u_i, i = 1,\dots 4, \\ r_1(\sigma) = r_2(\sigma) = r_5(\rho), \\ r_1'(\sigma) + r_2'(\sigma) - r_5'(\rho) = 0, \\ r_3(0) = r_4(0) = r_5(0), \\ r_3'(0) + r_4'(0) + r_5'(0) = 0. \end{cases} \tag{89}$$

We perform a similar analysis as in Section 4 and therefore omit the details. We obtain

$$\begin{aligned} r_1^\rho(x) &= \frac{1}{\ell}(u_1 - \frac{1}{4}\sum_{i=1}^4 u_i)x + \frac{1}{4}\sum_{i=1}^4 u_i \\ &\quad - \frac{\rho}{2\ell^2}\left\{[\frac{1}{2}\cos\alpha + 1](u_2-u_1) + (2-\cos\alpha)(u_1 - \frac{1}{4}\sum_{i=1}^4 u_i)\right\}(x-\ell) \\ &= r_1^0(x) \\ &\quad - \frac{\rho}{2\ell^2}\left\{[\frac{1}{2}\cos\alpha + 1](u_2-u_1) + (2-\cos\alpha)(u_1 - \frac{1}{4}\sum_{i=1}^4 u_i)\right\}(x-\ell), \end{aligned}$$

$$r_2^\rho(x) = r_2^0(x)$$
$$- \frac{\rho}{2\ell^2}\left\{([\frac{1}{2}\cos\alpha + 1](u_1 - u_2) + (2 - \cos\alpha(u_2 - \frac{1}{4}\sum_{i=1}^{4} u_i)\right\}(x-\ell),$$
$$r_3^\rho(x) = r_3^0(x)$$
$$- \frac{\rho}{2\ell^2}\left\{[1 - \frac{1}{2}\cos\alpha](u_2 - u_1) + (2 - \cos\alpha(u_2 - \frac{1}{4}\sum_{i=1}^{4} u_i)\right\}(x-\ell),$$
$$r_4^\rho(x) = r_4^0(x)$$
$$- \frac{\rho}{2\ell^2}\left\{[1 - \frac{1}{2}\cos\alpha](u_1 - u_2) + (2 - \cos\alpha)(u_1 - \frac{1}{4}\sum_{i=1}^{4} u_i)\right\}(x-\ell).$$

In order to calculate the energy we use the Steklov-Poincaré mapping and multiply by $r_i(\ell)$.

As before, the calculations can be done for scalar problems as well as for vectorial in-plane models. We dispense with the display of the lengthy formulae. Instead, we give two different scenarios for topological derivatives.

EXAMPLE 5.2 *In the scalar case we may set $u_1 = u_2$ and $u_3 = u_4 = 0$, i.e., we apply Dirichlet conditions at the ends of edges 3 and 4 and pull at the end of the edges 1 and 2 by the same amount. This results in:*

$$\langle S^\rho u, u\rangle = \langle S^0 u, u\rangle - \frac{\rho}{2\ell^2}(2 - \cos\alpha)u^2. \tag{90}$$

Obviously, the introduction of a new edge is enhanced. One obtains a decomposition into two multiple nodes with edge degree 3

EXAMPLE 5.3 *In the second example we take the planar model and set $u_1 = ue_1, u_2 = ue_2$ and again $u_3 = 0 = u_4$. Now we obtain*

$$\langle S^\rho u, u\rangle = \langle S^0 u, u\rangle - \frac{3\rho}{4\ell^2}\left[\cos(\alpha)(\cos^2\alpha + \frac{2}{3}\cos\alpha - \frac{4}{3})\right]u^2. \tag{91}$$

For small enough angles α (e.g. $0 < \alpha < \pi/6$) the expression with ρ, i.e. the topological derivative of the energy becomes negative. This shows that in the planar situation, the opportunity to create an additional edge depends on the angles between the edges 1 and 2.

Obviously, the examples above can be generalized to more general networks including distributed loads and obstacles. It is also possible to extend this analysis to 3-d networks. This is subject to a forthcoming publication.

6. Conclusion and further work

We have provided a first sensitivity-analysis of topological changes in continuous networks carrying a process described by an elliptic model. The analysis is

performed for scalar and vectorial planar graphs representative of heat flow (after proper transformation with respect to time) and mechanical networks. As this work is purely analytical, a numerical study will be presented elsewhere. Moreover, 3-d networks, which are obviously more realistic, will by discussed in a forthcoming publication. The analysis initiated here will be extended to bilevel optimization problems, where the sensitivity analysis (upper level) is applied to an optimal structure with the optimization (lower level) being performed with respect to thickness and material properties. All this will be important in lightweight- and nano-structures as well as in macro- and micro-flow networks.

References

Allaire, G., Gournay, F., Jouve, F. and Toader, A.M. (2004) Structural optimization using topological and shape sensitivities via a level set method. Ecole Polytechnique, R.I. 555.

Amstutz, S. (2003) Aspects théoriques et numériques en optimisation de forme topologique. PhD Thesis, Toulouse.

Bernot, M., Caselles, V. and Morel, J.M. (2007/2008) *Branched Transportation Networks.* Springer-Verlag.

Buttazzo, G. (2005) Optimization problems in the theory of mass transportation. *Boll. Unione Mat. Ital.* **9/1**, 401-427.

De Wolf, D. and Smeers, Y. (1996) Optimal dimensioning of pipe networks with application to gas transmission networks. *Oper. Res.* **44**(4), 596-608.

Durand, M. (2006) Architecture of optimal transport networks, *Physical Review E* **73**, 016116.

Hintermüller, M.A. (2004) A combined shape-Newton topology optimization technique in real-time image segmentation. In: *Real-Time PDE-Constrained Optimization*, Comput. Sci. Eng., SIAM.org, 253-274.

Kočvara, M. and Zowe, J. (1996) How mathematics can help in design of mechanical structures. In: Griffiths, D.F. et al., eds., *Numerical Analysis 1995. Proceedings of the 16th Dundee conference on numerical analysis*, University of Dundee, UK, June 27-30, 1995. Longman: Harlow. *Pitman Res. Notes Math. Ser.* **344**, 76-93.

Lagnese, J.E., Leugering, G. and Schmidt, E.J.P.G. (1994) *Modeling, Analysis and Control of Dynamic Elastic Multi-link Structures.* Birkhäuser, Boston, *Systems and Control: Foundations and Applications.*

Lagnese, J.E. and Leugering, G. (2004) *Domain Decomposition Methods in Optimal Control of Partial Differential Equations.* ISNM. *International Series of Numerical Mathematics* **148**. Birkhäuser, Basel.

Masmoudi, M., Pommier, J. and Samet, B. (2005) The topological asymptotic expansion for the Maxwell equation and some applications. *Inverse Problems* **21** (2), 547-564.

Mróz, Z. and Bojczuk, D. (2003) Finite topology variations in optimal design of structures. *Struc. Multidisc. Optim.* **25**, 1-21.

Novotny, A., Feij'oo, R., Taroco, E. and Padra, C. (2007) Topological sensitivity analysis for three-dimensional linear elastic problem. *Comp. Meth. Appl. Eng.* **196**, 41, 4354-4364.

Rozvany, G.I.N. (1998) Topology optimization of multi-purpose structures. *Math. Methods Oper. Res.* **47** (2), 265-287.

Sokolowski, J. and Zochowski, A. (1999) Topological derivatives for elliptic problems. *Inverse Problems* **15**, 123-134.